From Exponential Growth to Saturation: An Instability Dissected in Phase-Space

Jihad Rachid Touma

Department of Physics

American University Of Beirut

Beirut, Lebanon

Partners in Crime

- Mher Kazandjian (AUB, Lebanon)
- S. Sridhar (RRI, Bangalore, India)
- Scott Tremaine (Princeton, USA)

Plan (roughly)

- Preamble
- Instability
- Dissection
- Summary
- Plan (actually)

The "Double" Nucleus of M31: Observations, Hypotheses, Models and Implications

FIG. 7.—*HST* WFPC2 color image of M31 constructed from *I*-band, *V*-band and 3000 Å band PSF-deconvolved images obtained by Lauer et al. (1998). The left brightness peak (with embedded blue star cluster) is P2; the right peak is P1. The *I*- and *V*-band images were substepped by half of a PC pixel, so the scale is $0\farcs0228$ pixel^{-1}. The 3000 Å image was not substepped; we matched it to the *I*- and *V*-band images by interpolation.

The "Double" Nucleus of M31: Observations, Hypotheses, Models and Implications

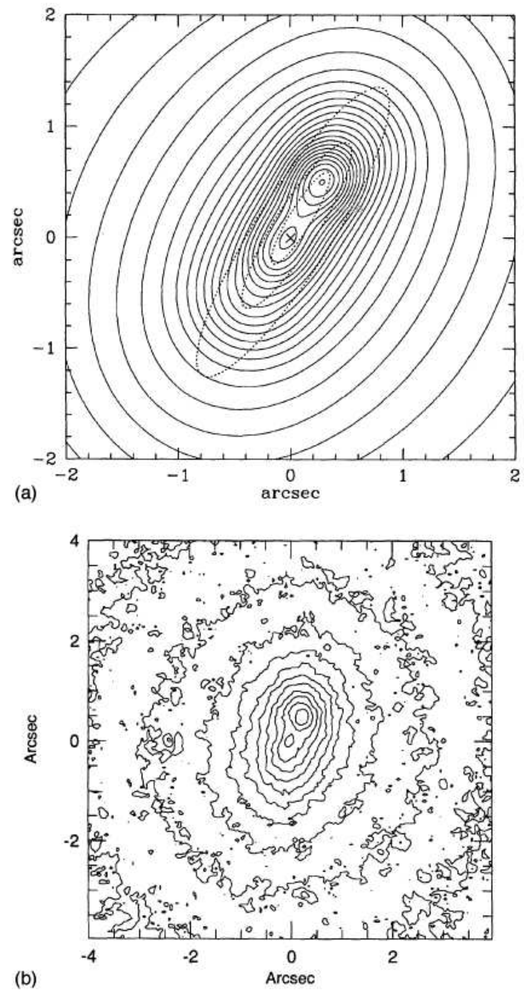

FIG. 2. (a) Contour map of the surface brightness of the best-fit model. The contour interval is $0^{m}.1$, and the vertical axis points 70° counterclockwise from north. The origin, which coincides with the black hole at $P2$, is marked by a cross, and the projected locations of the three ringlets in Eq. (2) are shown as dotted lines. (b) Deconvolved V-band surface-brightness contours of the nucleus of M31 (Fig. 2 of L93). The orientation and origin are the same as in (a) but the contour interval of $0^{m}.25$ is larger and a larger area is shown.

The "Double" Nucleus of M31: Observations, Hypotheses, Models and Implications

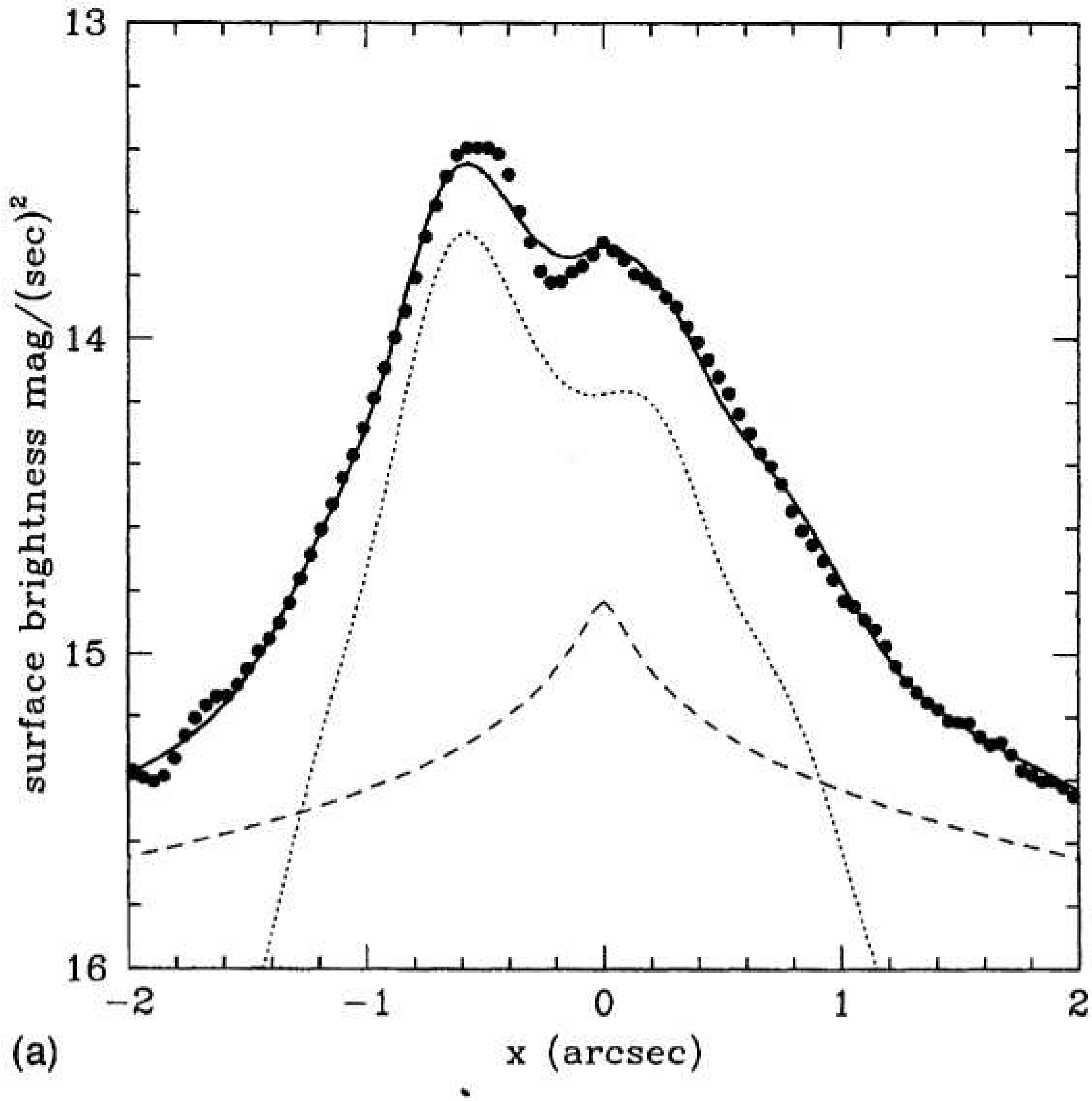

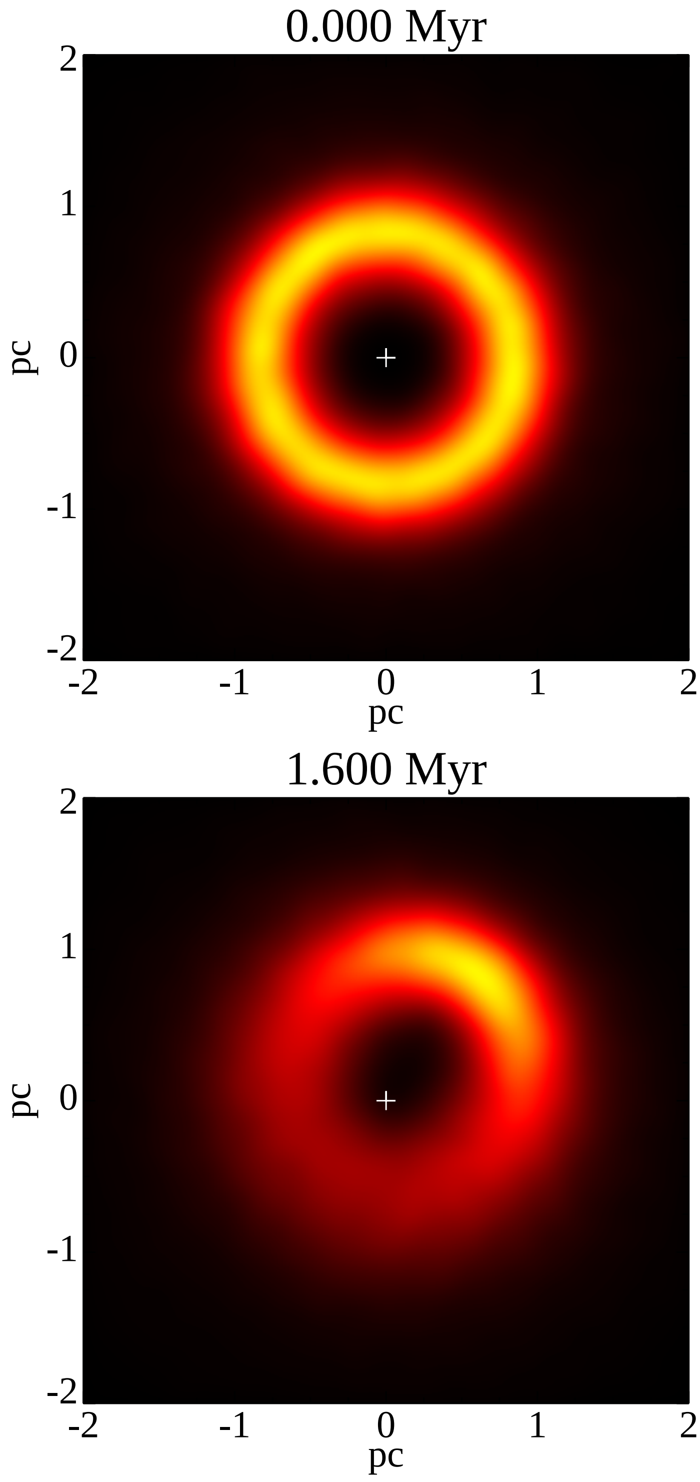

Figure 1: Before and After

Two Counter-Rotating Rings

- Start with two softened counter-rotating Keplerian rings, with angular momenta, $L_p = m_p\sqrt{GM_\bullet a_p(1-e_p^2)}$ and $L_r = -m_r\sqrt{GM_\bullet a_r(1-e_r^2)}$;
- Of course both secular energy, and total angular momentum, $L_T = L_p + L_r$ are conserved;
- A positive torque exerted by p on r would increase r's angular momentum, making L_r tend to zero, hence increasing r's eccentricity;
- An equal and opposite (hence negative) torque exerted by r on p would decrease p's angular momentum, making L_p tend to zero, hence increasing r's eccentricity;
- The CR instability requires that such a configuration is maintained for sufficiently long to bring about significant growth in eccentricities; maintaining such a configuration would require that rings precess with neighboring frequency, in the same direction, with increasing eccentricity: Such a tuning is provided by softening(heat)!

Numerical Clusters

- Black Hole, $10^8 M_\odot$, dominating cluster, $10^7 M_\odot$, perturbed by various counter-rotating perturbers, $10^5 - -5 10^6 M_\odot$;
- Cluster: thin Kuzmin disk (ring) radial scale of 1pc, with vertical $sech^2$ profile with 0.1pc, typical $\sigma_v \simeq 200$km/s;
- Perturbers: Counter-rotating: ring (both overlapping and not, coplanar, inclined), IMBH (various configurations).
- $10^4 - -10^6$ particles, softening length of 10^{-3}pc for particle-particle interactions, and 10^{-5}pc for particle-SMBH interactions;
- Parallel runs on cluster of 8-36 procs, with tree code (Gadget's parallel version), pushed to its limits, errors of 10^{-4} and 10^{-5} in energy and angular momentum respectively, over 1 Myr calculations ($10 T_{prec}$).

Axisymmetric to Eccentric

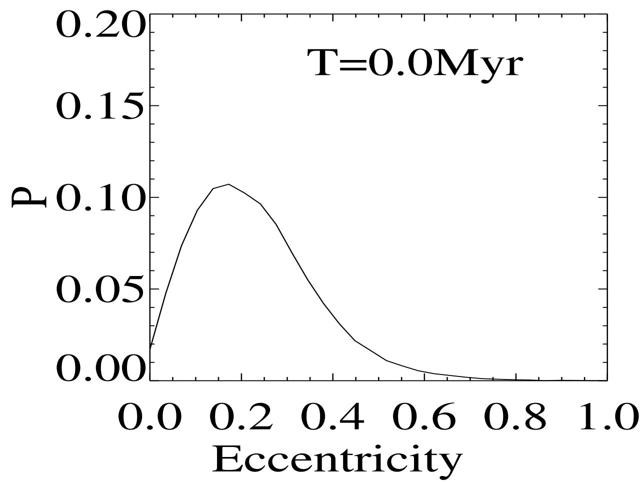

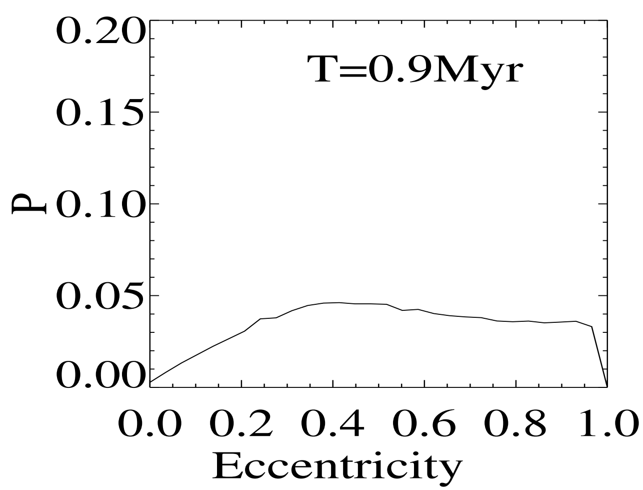

Puffing up a Thin Disk

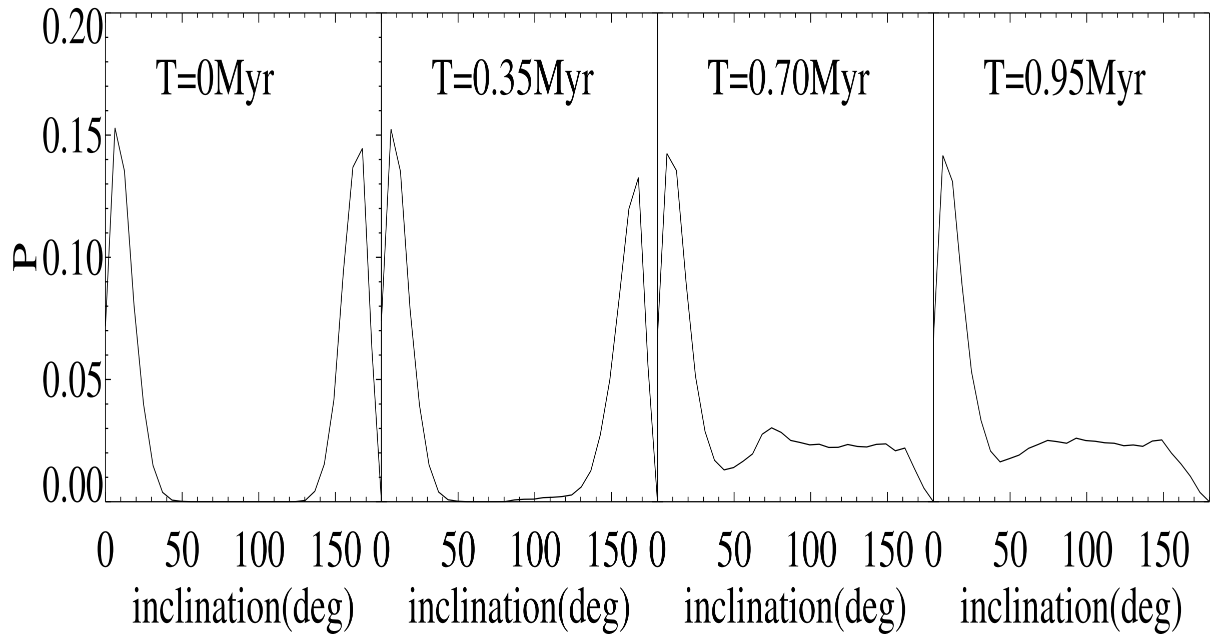

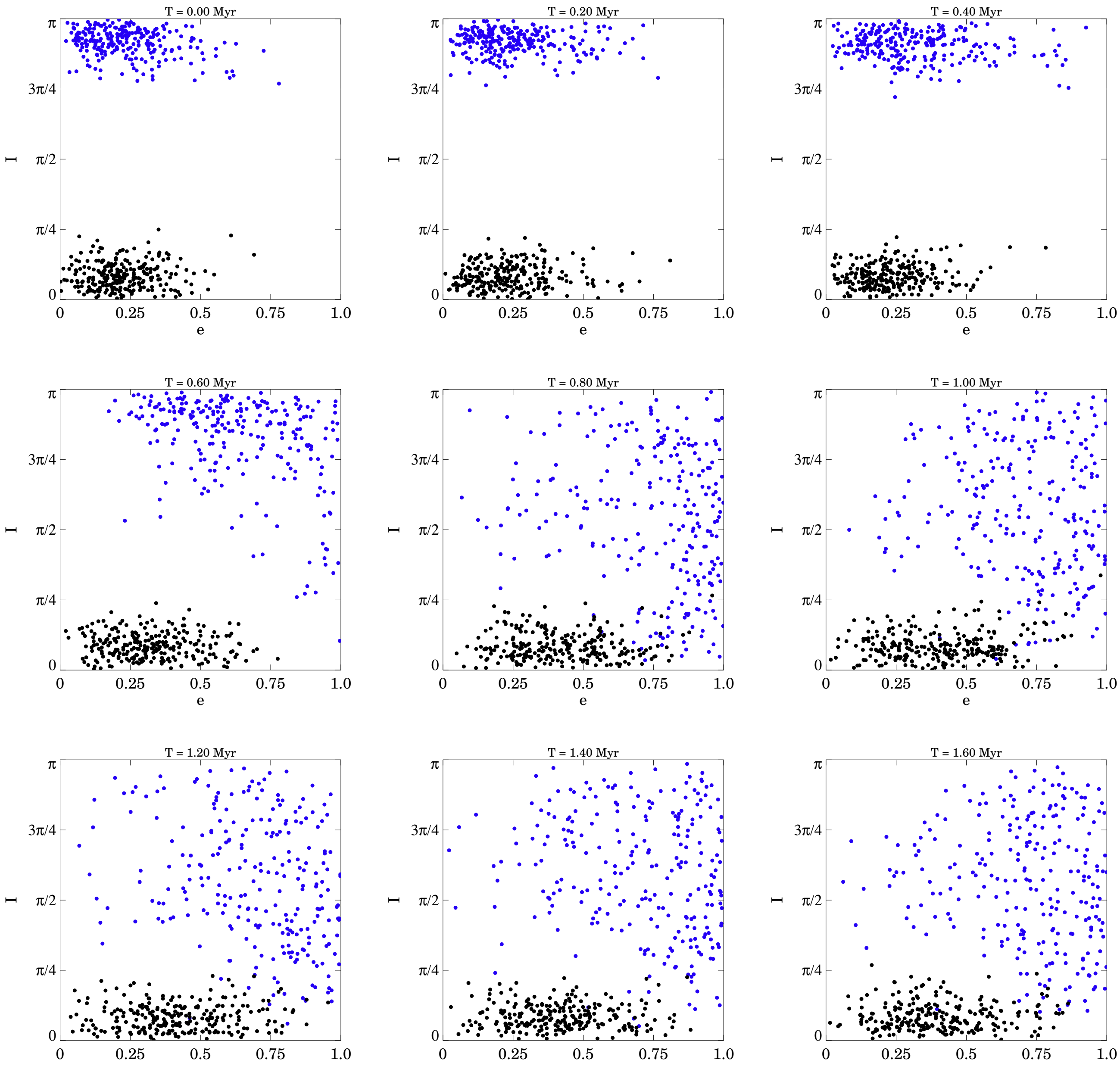

Figure 1: Eccentricity-Inclination Evolution

Mode Relaxation as Function of SMBH Softening

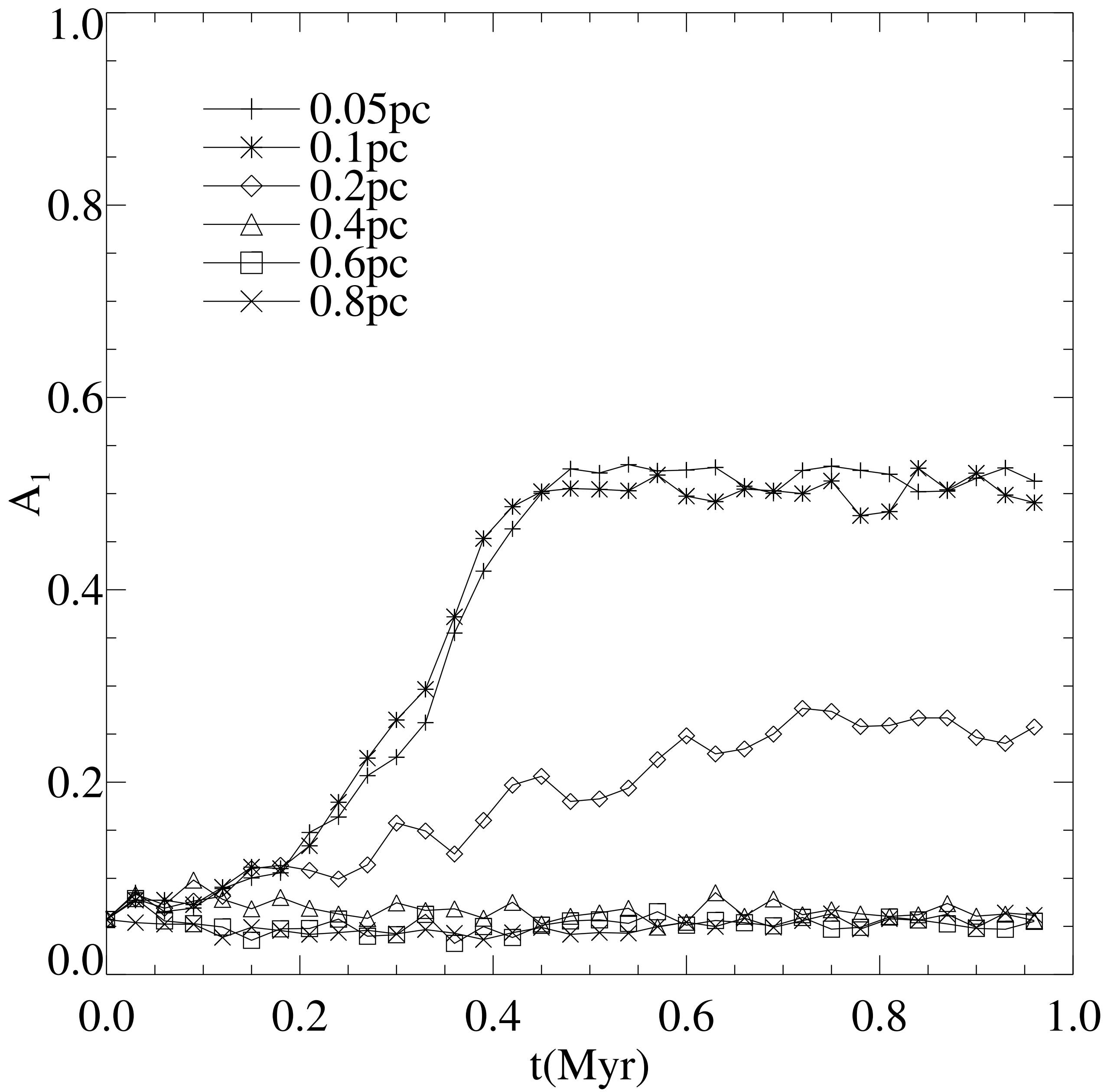

Averaged (secular), self-consistent, collisionless dynamics

Evolution governed by CBE-Poisson system of equations:

$$\frac{\partial f}{\partial t} + \mathbf{v} \cdot \frac{\partial \mathbf{f}}{\partial \mathbf{r}} - \nabla \phi \cdot \frac{\partial \mathbf{f}}{\partial \mathbf{v}} = \mathbf{0}$$

where: $\phi(\mathbf{r}, \mathbf{t}) = \phi_{\mathbf{self}}(\mathbf{r}, \mathbf{t}) + \phi_{\mathbf{ext}}(\mathbf{r}, \mathbf{t})$,

$$\phi_{self}(\mathbf{r}, \mathbf{t}) = -\mathbf{G} \int \mathbf{d^3 r' d^3 v'} \frac{\mathbf{f(r', v' t)}}{|\mathbf{r} - \mathbf{r'}|}$$

and $\phi_{ext}(\mathbf{r}, \mathbf{t}) = \frac{-\mathbf{G M_\bullet}}{\mathbf{r}} + \phi_{\mathbf{c}}(\mathbf{r}, \mathbf{t})$

- Black-Hole dominated dynamics, hence essentially Keplerian motion perturbed by cluster potential. Replace orbits by rings, with mass distributed inversely proportional to time spent on orbit (Averaging, Gauss)
- Consequence of Averaging: $L \sim \sqrt{GM_\bullet a}$ conserved, leaving precession (periapsis, node) and eccentricity/inclination dynamics of Gaussian ring, in averaged cluster potential: $f_{ave}(L, G, H, g, h, t)$

Secular (Orbit Averaged), CBE-Poisson Dynamics

The three actions are:

- $I_a = \sqrt{GMa}$;
- $L_a = |\boldsymbol{r} \times \boldsymbol{v}|$, the magnitude of the orbital angular momentum;
- $L_{az} = (\hat{z} \cdot \boldsymbol{r} \times \boldsymbol{v})$, the z–component of the orbital angular momentum.

The angles conjugate to them:

- w_a, the orbital phase;
- g_a, the angle to periapse from the ascending node;
- h_a, the longitude of the ascending node.

In these Variabes:

$$H_{kepler}(I_a) = -1/2(GM/I_a)^2$$

Trivial Dynamics:

- All variables constant except, w_a;
- w_a advancing at constant keplerian rate: $\Omega_k = (\partial H_k/\partial I_a) = (GM)^2/I_a^3$

Secular Collisionless Boltzmann

Consequences on Forces:

- Potential: $\Phi(I,\, L,\, L_z,\, g,\, h,\, t) \;=\; -G \oint \frac{dw}{2\pi} \int d^3r'\, d^3v'\, \frac{F(I',L',L_z',g',h',t)}{|\boldsymbol{r}-\boldsymbol{r}'|}$
- Non Inertial Forces:

$$\boldsymbol{a}(t) = G \int d^3r\, d^3v\, F \frac{\hat{\boldsymbol{r}}}{r^2} \;=\; G \int dI\, dL\, dL_z\, dg\, dh F(I,\, L,\, L_z,\, g,\, h,\, t) \oint dw\, \frac{\hat{\boldsymbol{r}}}{r^2}$$

which averages to zero over a Keplerian orbit!

Slow Dynamics, Equations:

$$\frac{dL}{dt} \;=\; -\frac{\partial\Phi}{\partial g}\,, \qquad \frac{dg}{dt} \;=\; \frac{\partial\Phi}{\partial L}\,; \qquad \frac{dL_z}{dt} \;=\; -\frac{\partial\Phi}{\partial h}\,, \qquad \frac{dh}{dt} \;=\; \frac{\partial\Phi}{\partial L_z}$$

Slow Dynamics, CBE:

$$\frac{dF}{dt} \;\equiv\; \frac{\partial F}{\partial t} \;-\; \frac{\partial\Phi}{\partial g}\frac{\partial F}{\partial L} \;+\; \frac{\partial\Phi}{\partial L}\frac{\partial F}{\partial g} \;-\; \frac{\partial\Phi}{\partial h}\frac{\partial F}{\partial L_z} \;+\; \frac{\partial\Phi}{\partial L_z}\frac{\partial F}{\partial h} \;=\; \frac{\partial F}{\partial t} \;+\; [\,F\,,\,\Phi\,] \;=\; 0$$

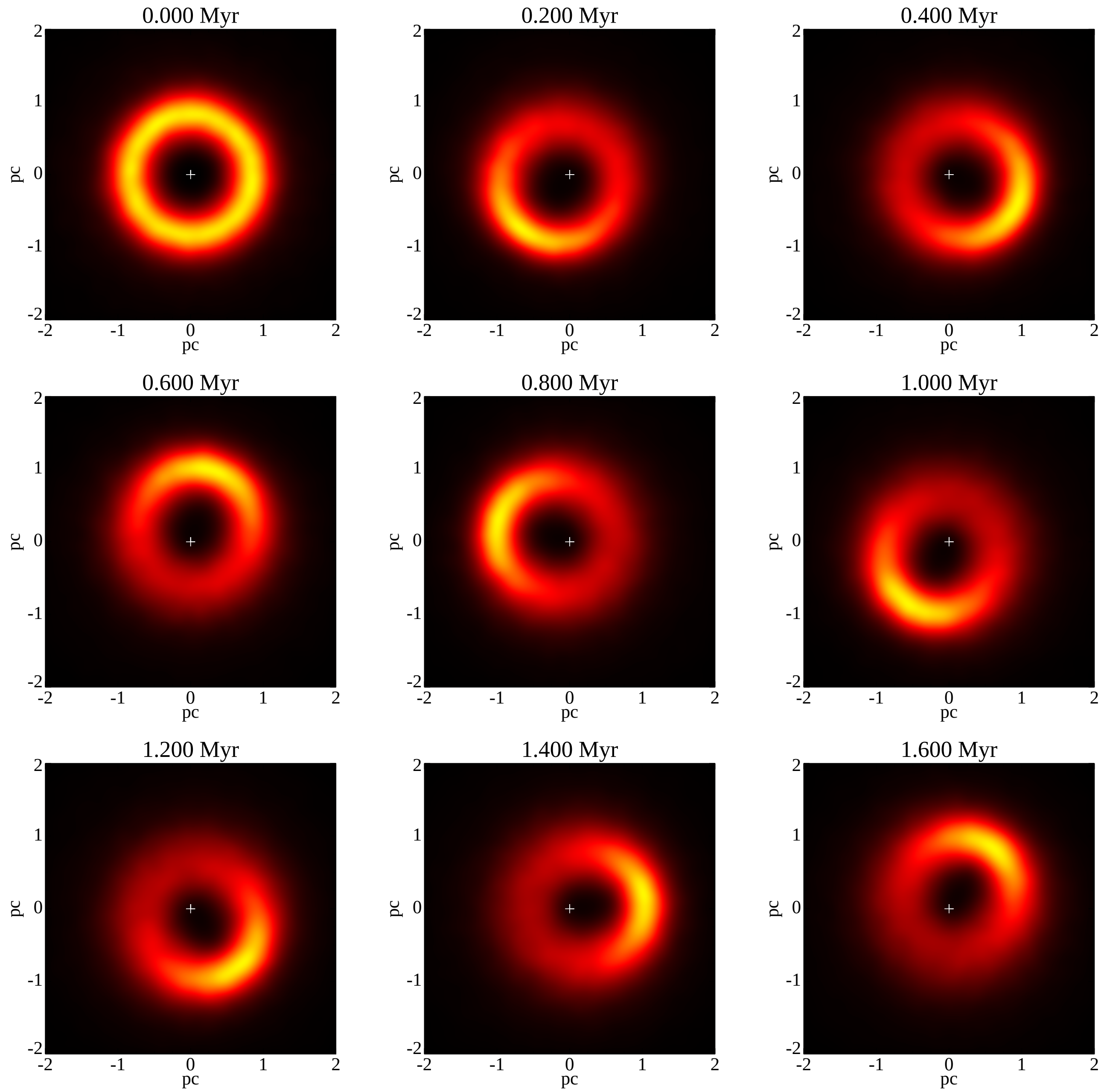

Figure 1: Instability in 2D: Density in Time

Single Particle Phase-Space

Restricting to Planar configurations:

- Cluster Mean Field: $\Phi(r,\theta,t) = \Phi_0(r,t) + \Phi_1(r,t)\cos[\theta + \phi(r,t)]$
- Single Particle Hamiltonian:: $H = \frac{v^2}{2} - \frac{GM}{r} + \Phi(r,\theta,t)$
- Softened Black Hole :: $H = \frac{v^2}{2} - \frac{GM}{r} + [\frac{GM}{r} - \frac{GM}{\sqrt{r^2+b^2}}] + \Phi(r,\theta,t)$
- Averaging over Keplerian ring: $x = a[\cos(g)(\cos(E) - \sqrt{1-e^2}) - l\sin(g)\sin(E)]$, $y = a[\sin(g)(\cos(E) - \sqrt{1-e^2}) + l\cos(g)\sin(E)]$;
- Averaged Hamiltonian: $H_{ave} = \Phi_0(a,l,t) + \Phi_1(a,l,t)\cos(g) - \Omega(t)l$
- $\bar{\Phi}_0 \propto e^2$ undergoes slight variations; $\bar{\Phi}_1(a,l,t) \propto e$ increases significantly; $\Omega(t)$ increases to a maximum of $60 kms^{-1}pc^{-1}$, before saturating at half that value;

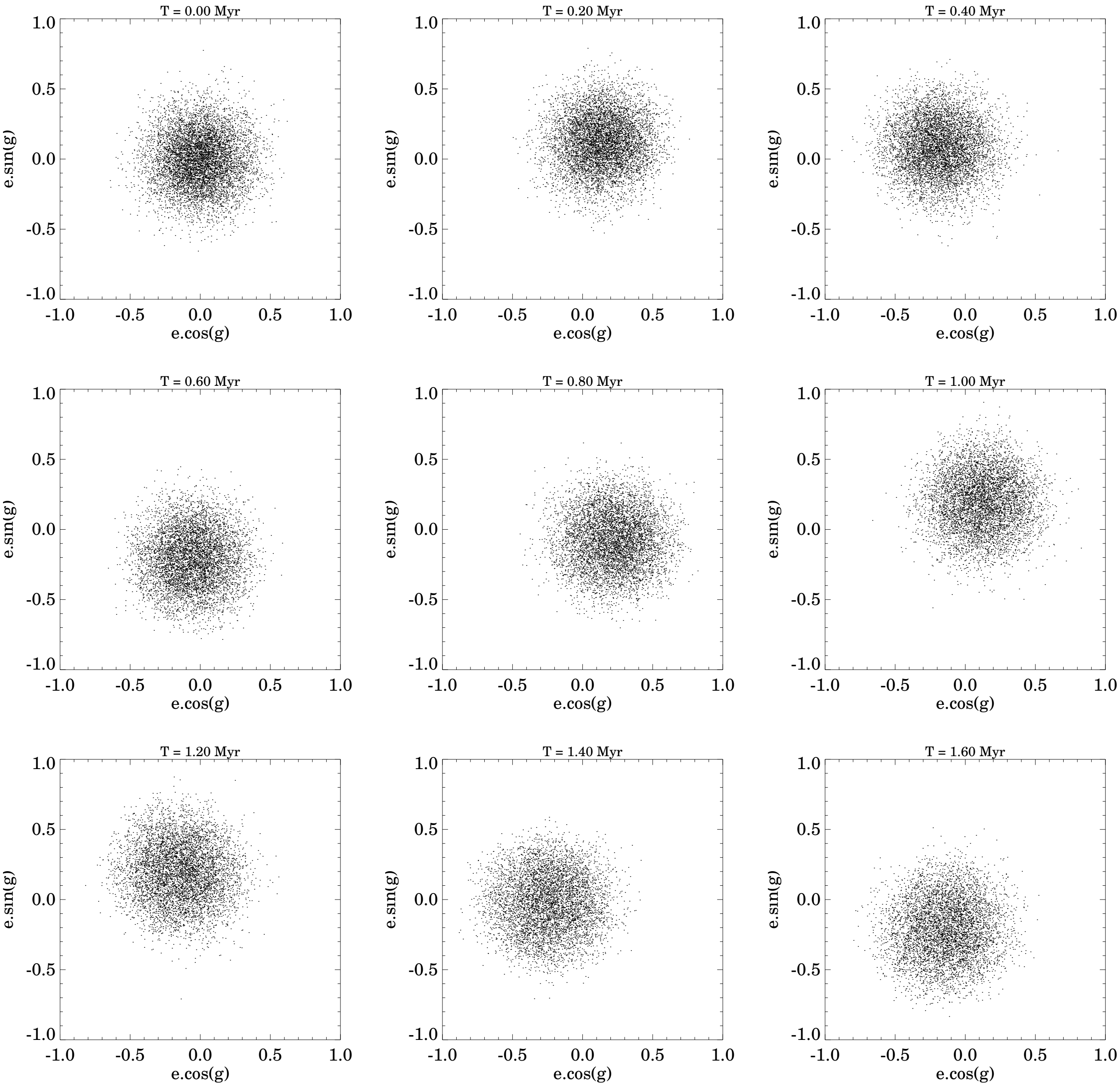

Figure 3: Instability in 2D: Prograde in xy-plane, $a = 0.9$pc

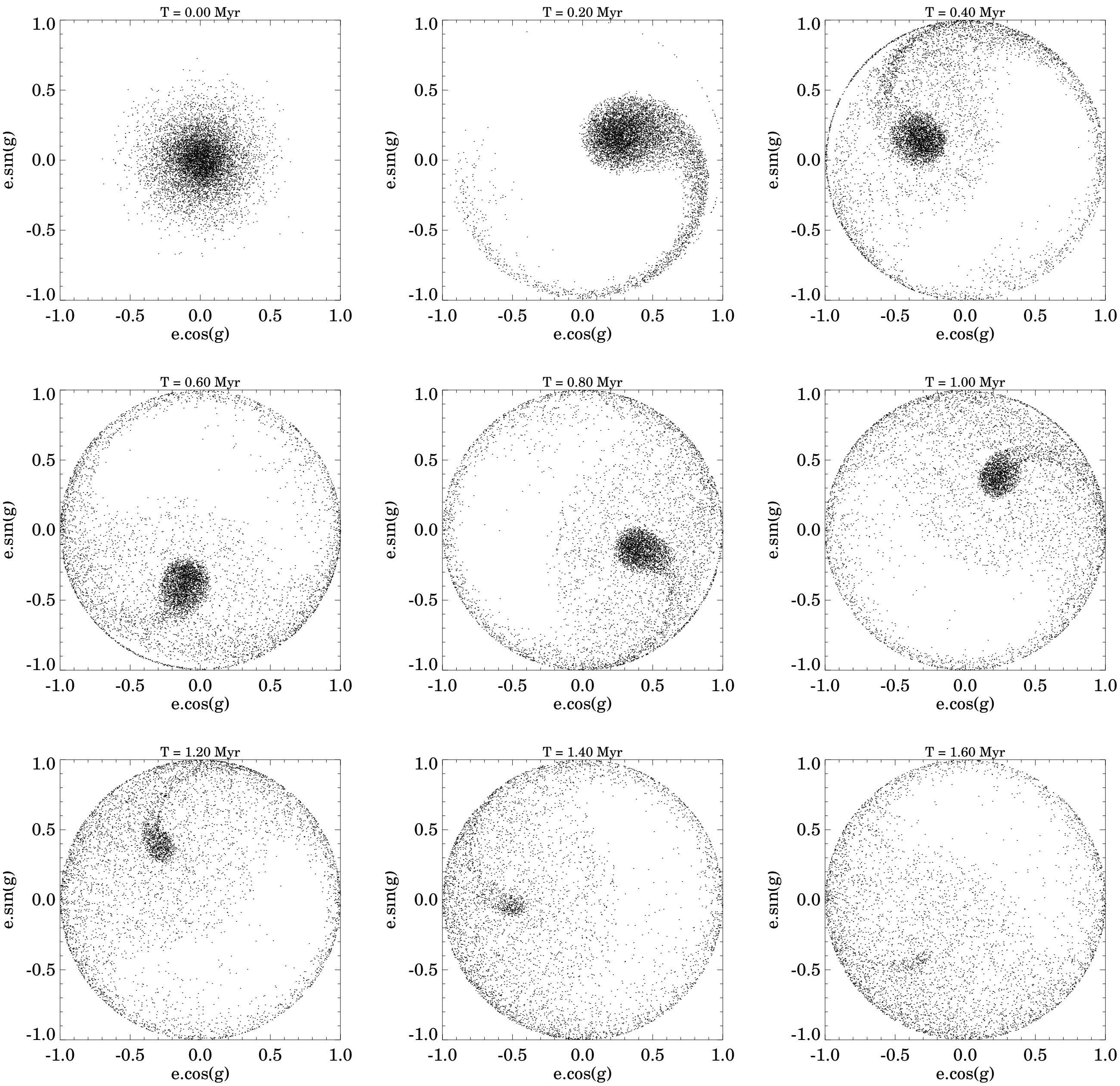

Figure 2: Instability in 2D: Retrograde in xy-plane, $a = 0.9$pc

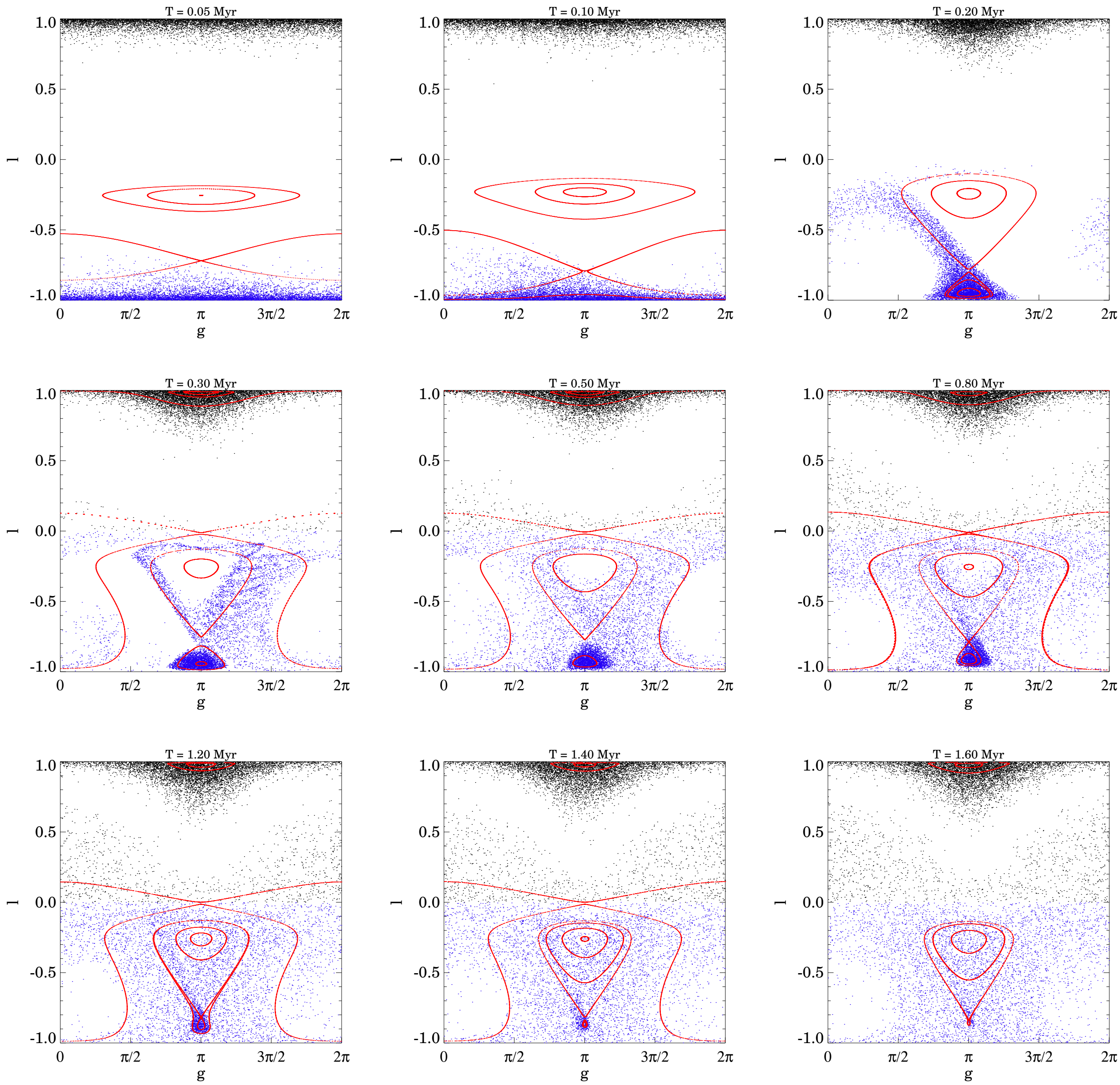

Figure 6: Instability in 2D: Retrograde in lg-plane, $a = 0.9$pc

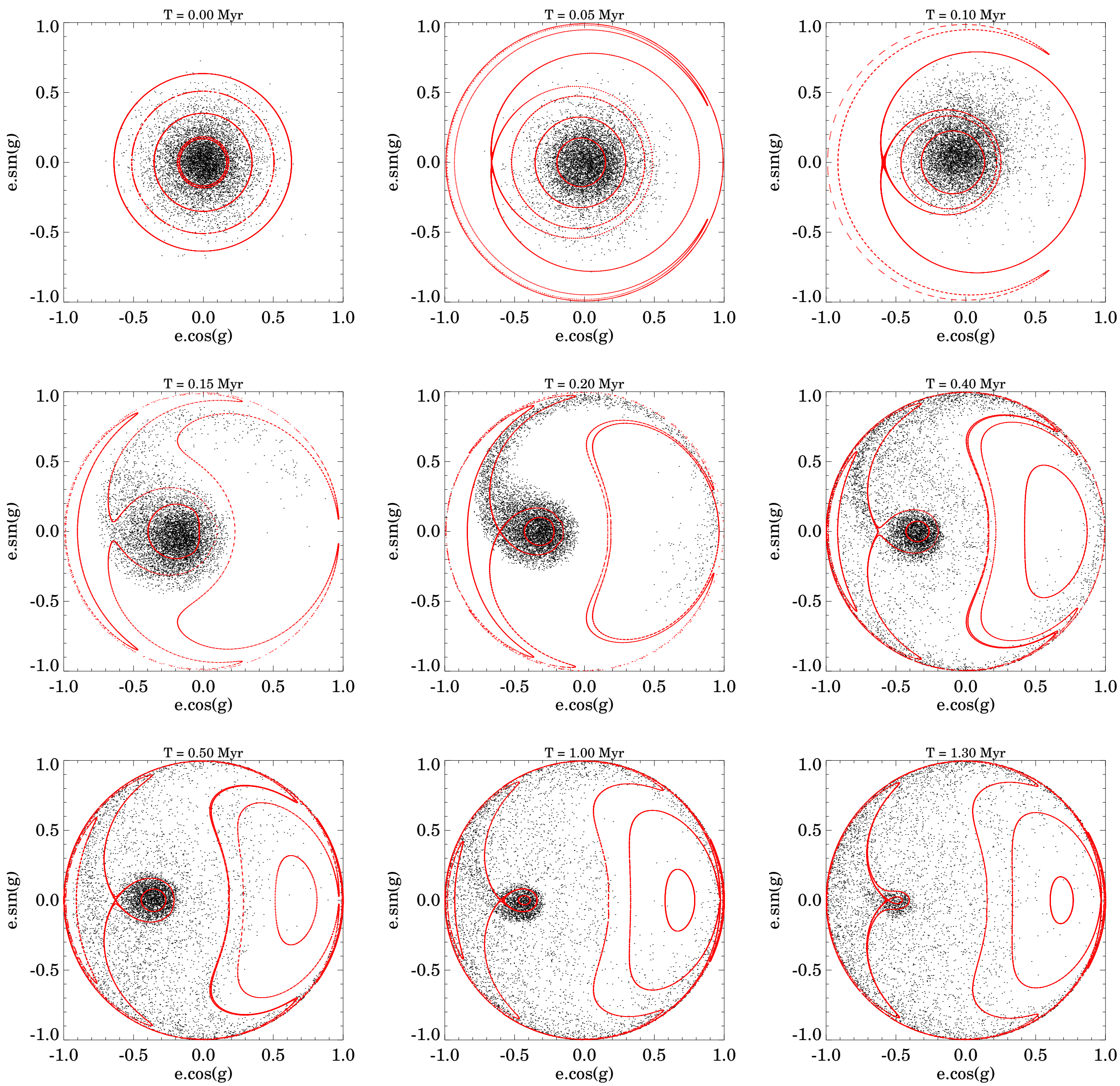

Figure 4: Instability in 2D: Retrograde in xy-plane, $a = 0.9$pc

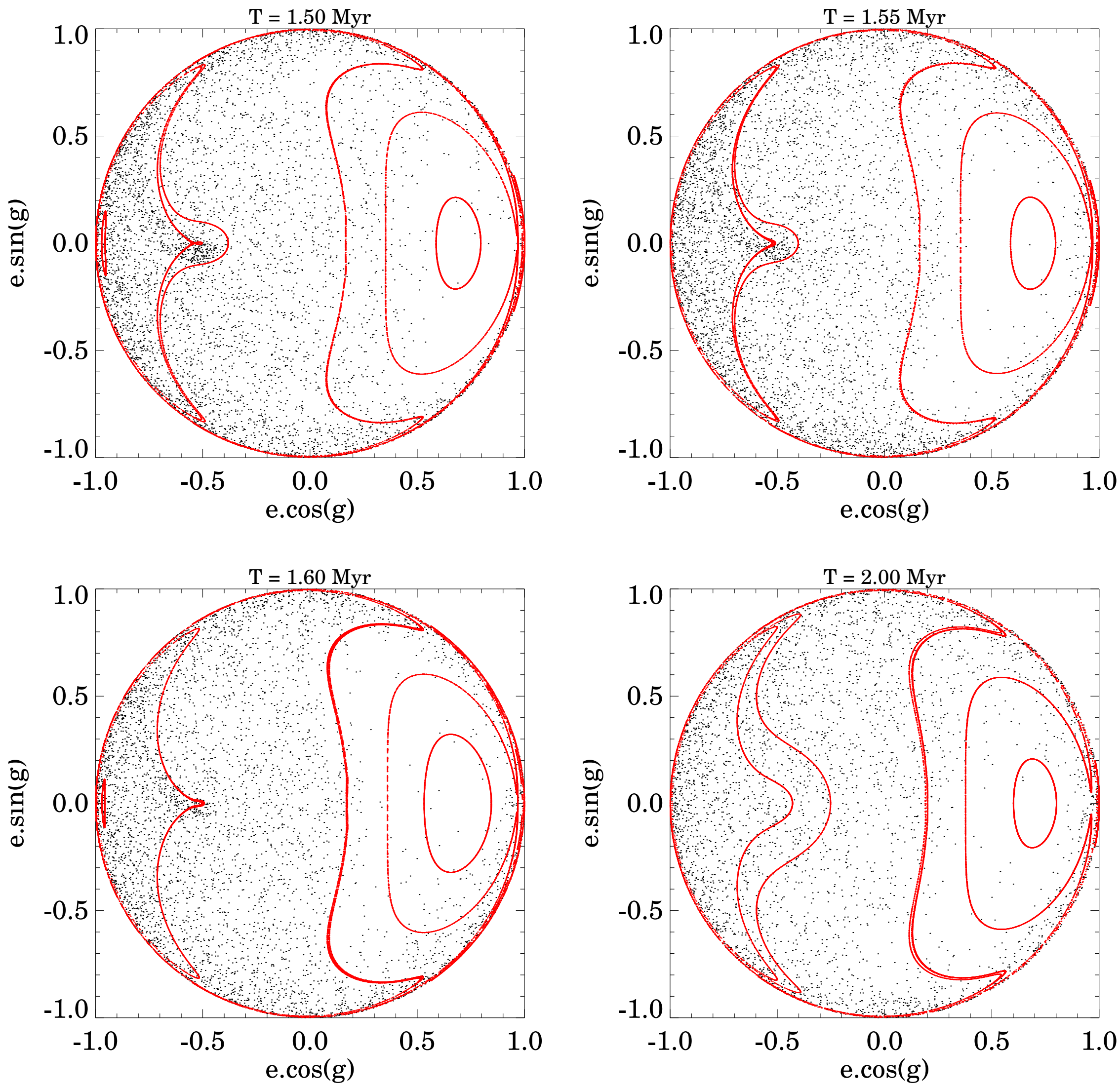

Figure 5: Instability in 2D: Retrograde in xy-plane, $a = 0.9$pc

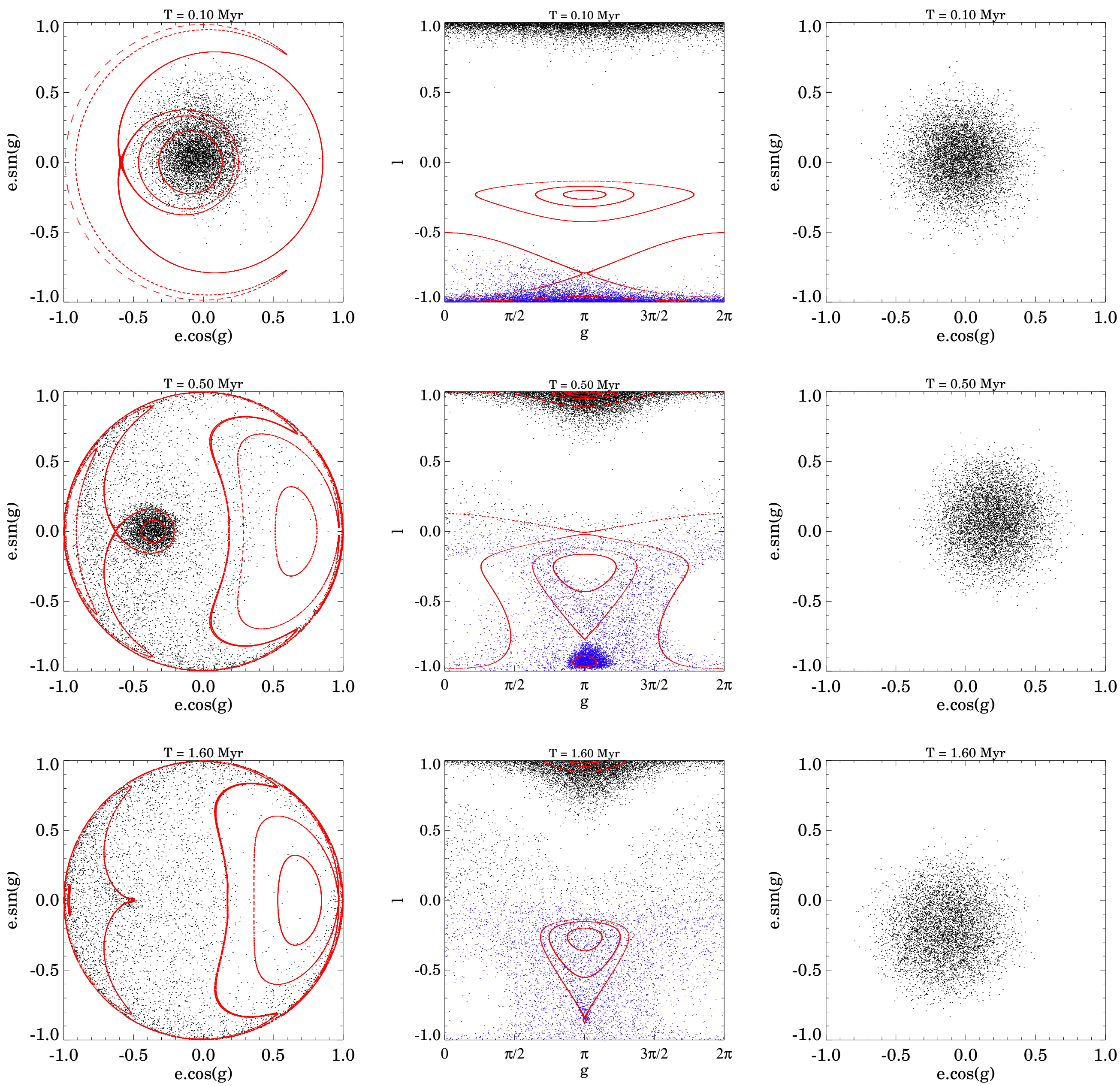

Figure 7: Instability in 2D: Sphere and Phase Plane $a = 0.9$pc

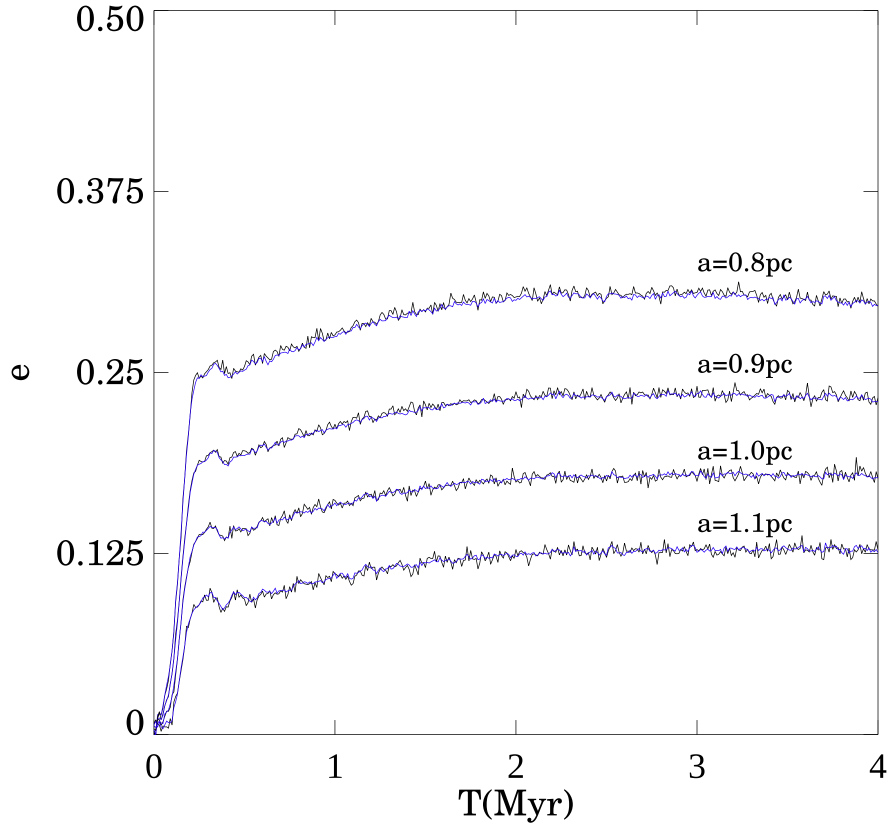

Figure 1: Particle Centroid vs Model Equilibrium: Prograde Population at various semi-major axis

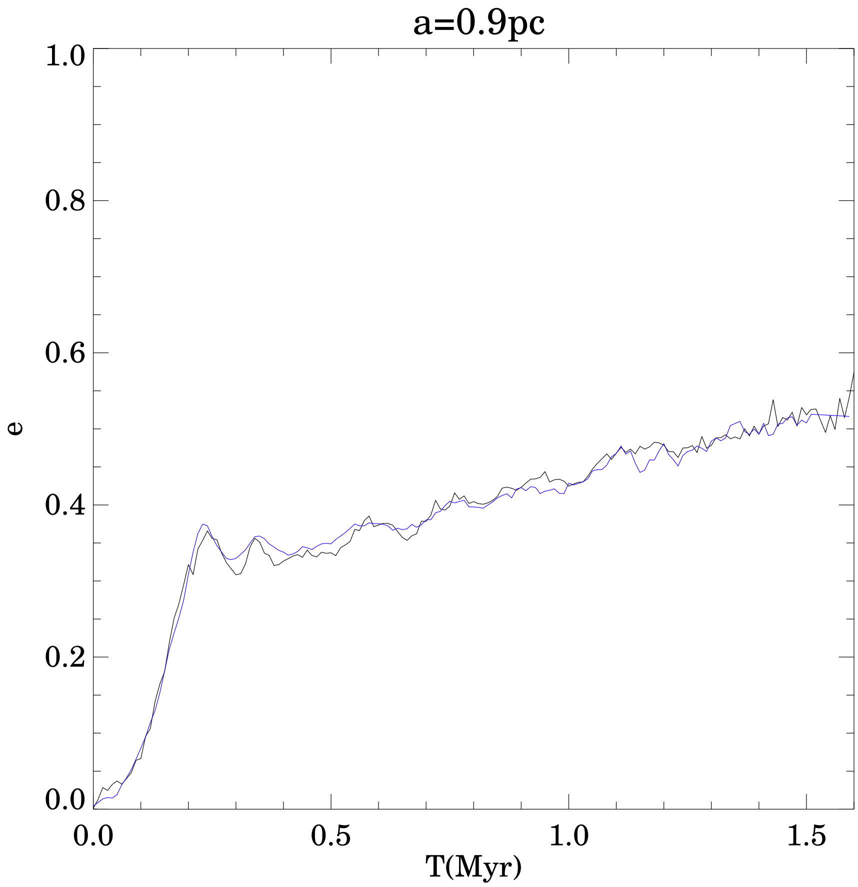

Figure 2: Particle Centroid vs Model Equilibrium: Retrograde Populations at $a = 0.9$ pc

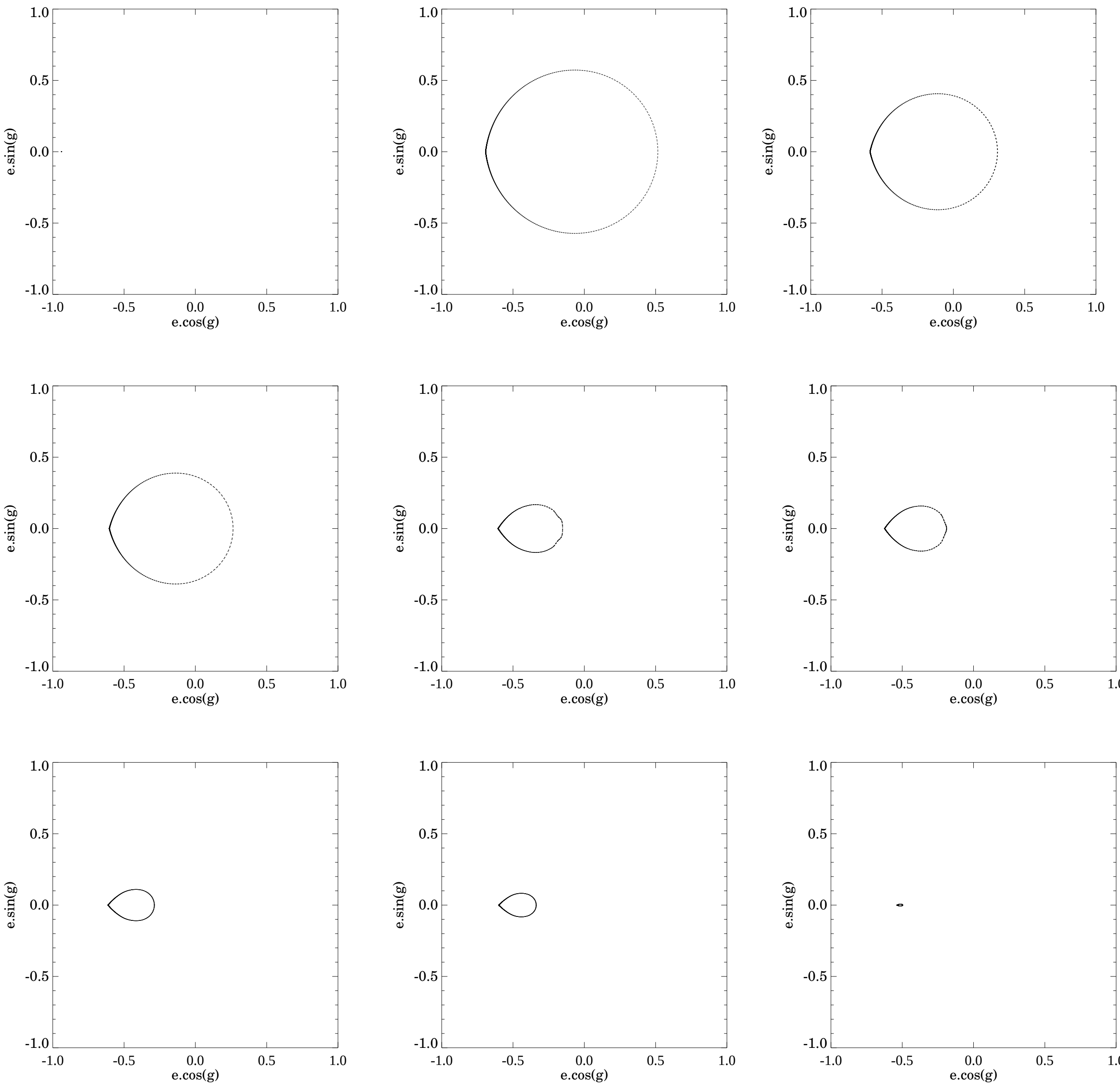

Figure 4: Instability in 2D: Equilibria and Separatrix

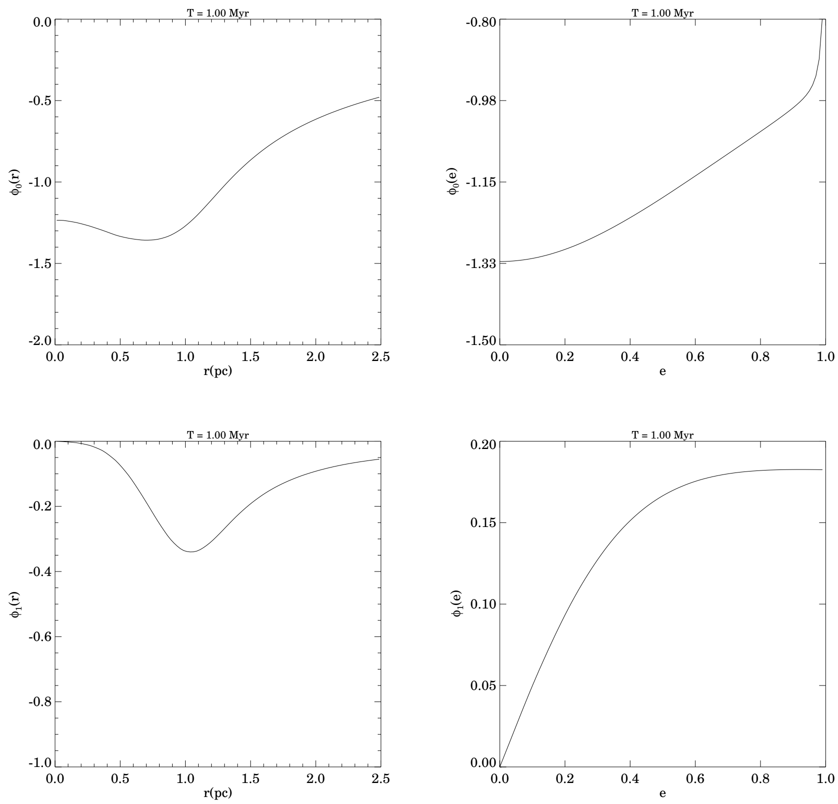

Figure 3: Φ_0 and Φ_1 before and after Averaging

Model Hamiltonian

- Averaged Hamiltonian: $H_{ave} = \Phi_0(a,l,t) + \Phi_1(a,l,t)\cos(g) - \Omega(t)l$
- For moderate eccentricity: $\bar{\Phi}_0 \propto e^2$, and $\bar{\Phi}_1(a,l,t) \propto e(\sqrt{1-l^2})$
- Model Hamiltonian: $H = -\frac{1}{2}f_0(t)l^2 + f_1(t)\sqrt{1-l^2}\cos(g) - \Omega(t)l$
- Adiabatic Limit: $t_{prec} \gg t_{growth}$, hence work with time-frozen Hamiltonian: $H_{freeze} = -\frac{1}{2}f_0 l^2 + f_1\sqrt{1-l^2}\cos g - \Omega l$
- Rescale by f_0: $\frac{H}{f_0} = -\frac{1}{2}l^2 + \alpha\sqrt{1-l^2}\,\cos g - \beta l$ with $\alpha = f_1/f_0$ and $\beta = \Omega/f_0$;
- One degree of freedom, with slowly varying parameters: $H_s = -\frac{1}{2}[l+\beta]^2 + \alpha\sqrt{1-l^2}\,\cos g$

Equations of Motion

Precession:

$$\frac{dg}{dt} = \frac{\partial H_s}{\partial l} = -l - \beta - \alpha \frac{l}{\sqrt{1-l^2}} \cos(g)$$

Torque (change in e):

$$\frac{dl}{dt} = -\frac{\partial H_s}{\partial g} = \alpha \sqrt{1-l^2} \sin g$$

or

$$\frac{dg}{dt} = -l - \beta - \alpha \frac{l}{e} \cos(g)$$

$$\frac{dl}{dt} = \alpha e \sin g$$

with $\alpha, \beta > 0$

Qualitative Features

- Increasing α: pattern is more lopsided, with stronger torques;
- Increasing β: faster pattern speed; prograde needs to decrease eccentricity (increase l) to keep up, if at all; and the reverse is true;
- Prograde ($l \geq 0$), aligned equilibrium: For increasing α (mode strength), e needs to increase to maintain equilibrium at fixed β; similarly if β were to decrease higher eccentricity would be required to maintain the equilibrium; indication of likelihood of capture;
- Increasing α: stronger mode, larger torques; positive torque increases eccentricity of retrograde ($l < 0, \Delta l > 0$), and decreases eccentricity of prograde orbit; negative torque works in reverse;

Qualitative Features

- Prograde ($l \geq 0$): retro-precession from axisymmetric mean field, modulated by contributions from lopsided field; for g around π (aligned orbits), pro-precession from $m = 1$ lump, and the possibility of reversing effect of axisymmetric Φ_0 to get a star to precess with prograde pattern;

- Retrograde ($l \leq 0$): pro-precession from axisymmetric mean field, modulated by contributions from lopsided field; for g around π (aligned orbits), retro-precession from $m = 1$ lump, and the possibility of reversing the effect Φ_0, to pull a star into retrograde precession;

Capture into and Escape From Resonance

Time variation of model parameters, $\alpha(t)$ and $\beta(t)$:

- Adiabatic Regime: variations slow when compared to orbital periods (precession due to $\Phi_0(t)$;
- A Sequence of time frozen Hamiltonians: Critical behavior around separatrices;
- Capture and Escape: Likelihood of excitation of $l > 0$ populations, likelihood of capture and excitation of $l < 0$;
- The Picture is modified by the self-consistent requirement in which $\alpha(t)$ and $\beta(t)$ are functions of the evolving distributions;

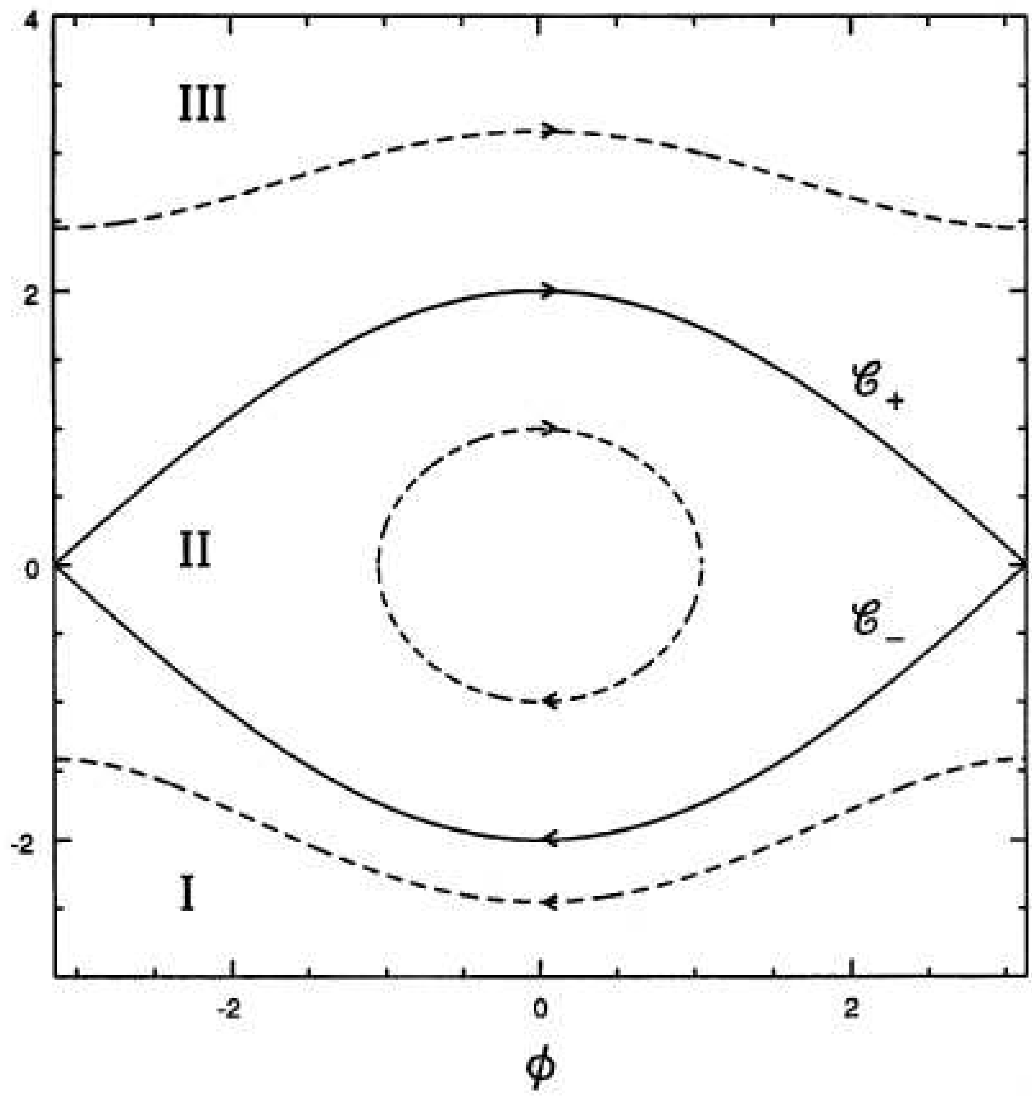

4
2
0
-2
III
II
I
$\mathscr{C}_+$
$\mathscr{C}_-$
-2
0
2
ϕ

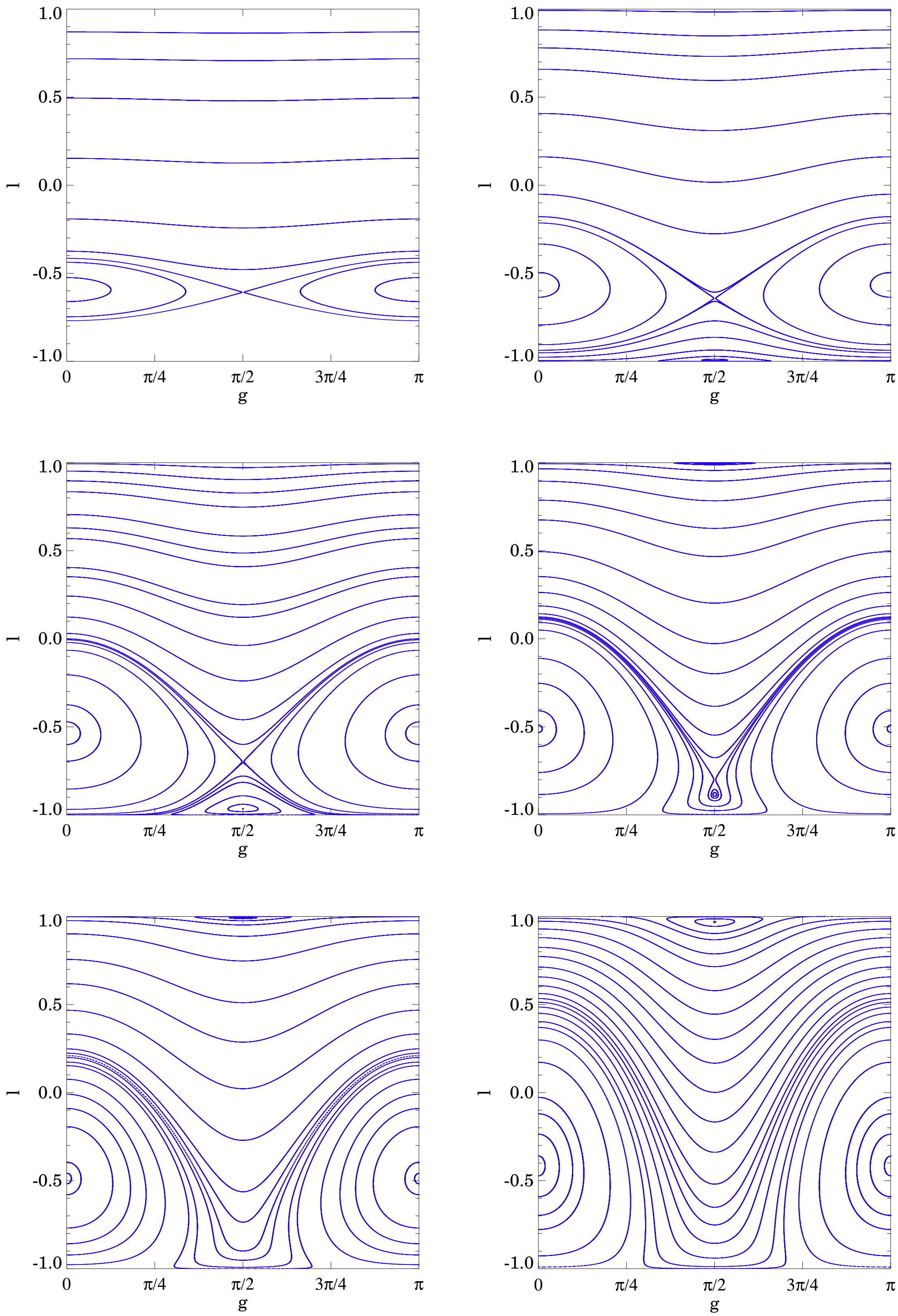

Figure 1: Model Hamiltonian: $\beta = 0.6$, and α varying between 0.01 and 0.4.

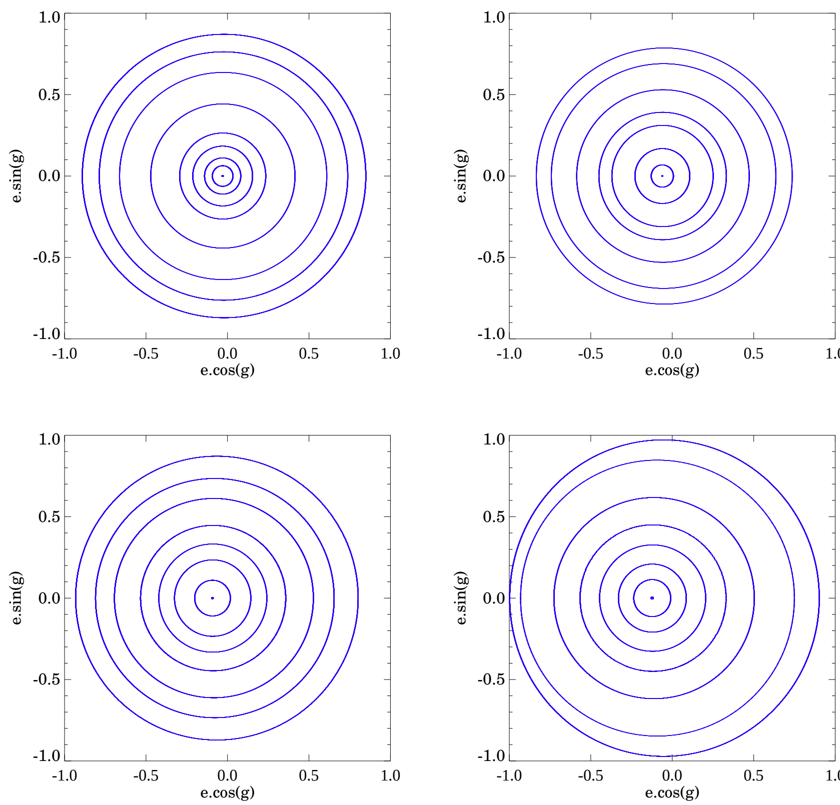

Figure 2: Model Hamiltonian: Prograde Dynamics for $\beta = 0.6$, and α varying between 0.01 and 0.4.

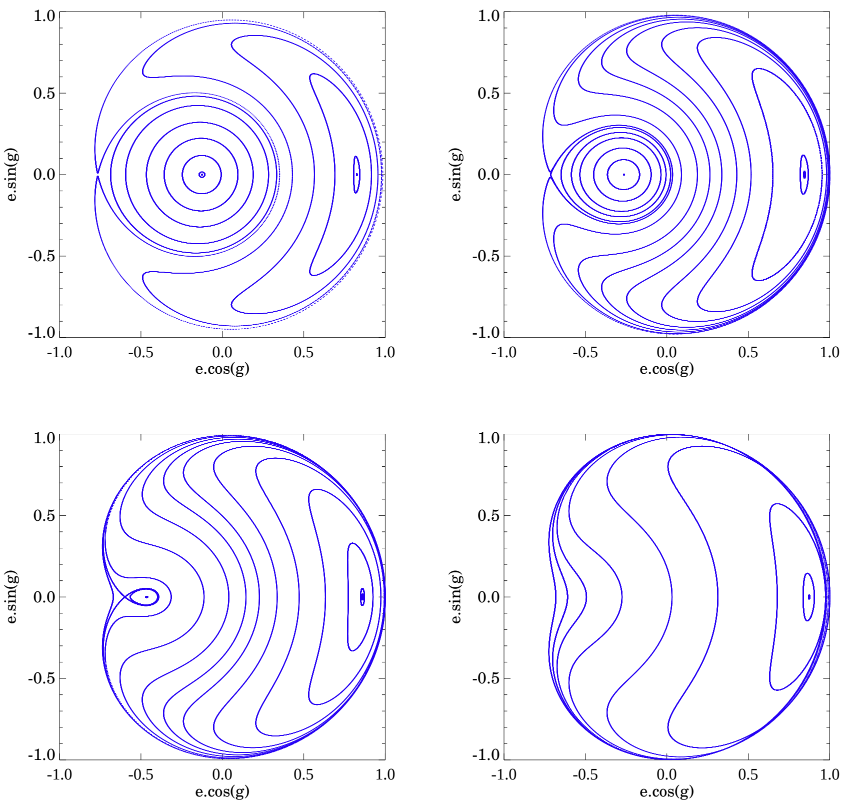

Figure 3: Model Hamiltonian: Prograde Dynamics for $\beta = 0.6$, and α varying between 0.01 and 0.4.

Summary

- Violent instabilities in Hot, Counter-Rotating, Stellar systems, which promote growth of eccentricities and inclinations on rather short timescales
- Unstable configurations saturate into puffy $m = 1$ equilibria: At least the m=1 part comes out naturally as a negative temperature thermodynamic equilibrium of counter-rotating clusters.
- Saturation is associated with the dispersal the (lighter), counter-rotating perturber: in 3D, via eccentricity/inclination instability; in 2D via filling of the full (prograde and retrograde) phase space.

Plan of Action

- In 2D: Construct a self-consistent model for the time-varying parameters that enter into our averaged, adiabatic dynamics;
- In 3D: Identify the source of eccentricity-inclination instability, and generalize current, 2D treatment, to the full 4D phase-space;
- For both limits: Study the workings of relaxation (mainly resonant) on the saturated mode;
- Secure the link between micro-canonical equilibria, and our global modes.